THE ASTROPHYSICAL JOURNAL, 546:569–575, 2001 January 1

OBSERVATION OF POLAR PLUMES AT HIGH SOLAR ALTITUDES

C. E. DEFOREST[1]
Southwest Research Institute, 1050 Walnut Street, Suite 426, Boulder, CO 80302; deforest@boulder.swri.edu
S. P. PLUNKETT
Universities Space Research Association, Naval Research Laboratory, Washington, DC 20375; plunkett@kreutz.nascom.nasa.gov
AND
M. D. ANDREWS
Raytheon ITSS, 4400 Forbes Boulevard, Lanham, MD 20706; andrews@louis14.nrl.navy.mil
Received 1999 July 22; accepted 2000 August 11

ABSTRACT

Using the Large-Angle Spectrometric Coronagraph (LASCO) aboard the *Solar and Heliospheric Observatory* (*SOHO*) spacecraft, we have imaged polar plumes extending 30 $R_\odot$ from disk center in the image plane and $\sim$45 $R_\odot$ in three-dimensional space, a factor of 2–3 farther than previous imaging measurements and well into the constant-velocity regime of wind flow. We find that the plumes maintain their overall linear morphology and density enhancement to at least this altitude range. Using LASCO photometry and a modeled cylindrical plume geometry, we derive the density excess within the plumes 30 $R_\odot$ above the Sun (in three dimensions). At this altitude, the plumes are (2–4) $\times$ 10^3 cm^{-3} above the background interplume density, with an estimated plasma β of order 300. The excess electron densities are a factor of 20–30 greater than the average total electron density estimates obtained from extrapolation of in situ measurements by *Ulysses* at 1 AU. The contrast between the high plume excess densities that we observe and the uniformity of the wind seen by *Ulysses* may best be explained by wind models that include horizontal mixing in the lower heliosphere between 45 $R_\odot$ and *Ulysses*'s altitude of $\sim$200 $R_\odot$.

Subject headings: solar wind — Sun: corona

1. INTRODUCTION

Polar plumes are magnetically unipolar, linear, high-density structures in the polar coronal holes of the Sun. Because unipolar magnetic flux concentrations in the coronal hole account for approximately 50% of the magnetic flux that threads the coronal hole (DeForest et al. 1997), plumes (which arise from some such concentrations) are tracers of a type of magnetic structure that fills nearly half of the solar system at solar minimum. Plumes were originally seen in white light (Saito 1965; Koutchmy 1977) but are also apparent in extreme ultraviolet (Bohlin, Sheeley, & Tousey 1975; Walker et al. 1988; Walker et al. 1993) and in soft X-rays (Ahmad & Webb 1978). They are denser and cooler than the surrounding media (DeForest et al. 1997; Walker et al. 1988), suggesting that they are heated principally at their bases (Wang 1994). They have been observed to extend through the coronal hole to altitudes of at least 10 $R_\odot$, expanding superradially with altitude throughout the corona (Kopp & Holzer 1976; DeForest et al. 1997; Suess et al. 1998) and into the constant-velocity, high-β regime that marks the lower portion of the heliosphere. Plumes last for about 1 day but have been observed to recur roughly daily for periods of up to 2 weeks in approximately the same location over the solar surface (DeForest 1998). The role of polar plumes in the solar wind has been a matter of debate (Walker et al. 1993; Habbal et al. 1995), in part because it is difficult to detect plume structure in the extremely faint corona at the high solar altitudes, where the plumes are thought either to fade or to merge with the solar wind.

The *Ulysses* spacecraft has observed density structures by sampling directly the high-speed solar wind about 1 AU over the solar poles; however, these structures do not appear to vary with latitude as would be expected for rigid plumelike structures rotating past the spacecraft (Poletto et al. 1996; Reisenfeld, McComas, & Steinberg 1999; McComas et al. 1995), and they appear to be much more homogeneous than the density structure of polar plumes at 2 $R_\odot$ (Feldman et al. 1996). The outflow rate in plumes is much lower than in the surrounding coronal hole. Recent observations by Banerjee et al. (2000) and Giordano et al. (2000) show that the plumes support at most a slow outflow that is consistent with the classical Parker (1958) solar wind solution, while the rest of the coronal hole flow is at least sonic at 2 $R_\odot$ (Cranmer et al. 1999). The question remains, if the plumes contain high-speed wind streams and hence impose structure on the high-speed solar wind, why is that structure not seen by *Ulysses*?

Possible explanations for the plumes' disappearance at high altitude include the Kelvin-Helmholtz two-stream instability (Parhi, Suess, & Sulkanen 1999) and cross-mode wave scattering near the Alfvénic point in the wind's acceleration (Kagashvili 1999). These mechanisms allow the plumes to contribute to the solar wind but cause their contribution to be distributed across radial lines by fluid-dynamic instabilities, spoiling their azimuthal structure above a critical altitude that is an adjustable parameter of each model. It has also been shown (DeForest 1998) that time variability in the plumes themselves may be sufficient to spoil the expected frequency signature of plumes in the *Ulysses* observations, even should their azimuthal structure persist to *Ulysses*'s altitude of approximately 1 AU, but time variability alone cannot account for the comparative

[1] This work was done in affiliation with Stanford University.

homogeneity of the *Ulysses* observations. If turbulent mixing by instabilities is in fact the mechanism at play, then the plumes should appear to fade above a critical altitude somewhere above 10 $R_{\odot}$.

There is currently some uncertainty (Woo 1996; Pätzold & Bird 1998; del Zanna, von Steiger, & Velli 1998) over how far the plumes actually extend into the interplanetary medium. Plumes have been observed in Thomson-scattered visible light to extend from the solar surface up to image-plane altitudes of 10–15 $R_{\odot}$ (DeForest et al. 1997), using the Large-Angle Spectrometric Coronagraph's (LASCO's) C-3 camera (Brueckner 1995). Woo (1996) reports observing plumes at solar altitudes as high as 40 $R_{\odot}$ in the image plane, using radio sounding of the corona with the *Ulysses* transponder beam, but several factors require clarification of this result. In particular, the timescale of the plumes' passage in the Woo result (1.0 days) is suspiciously similar to the diurnal rhythm of the Deep Space Network coverage that was used to make the measurement (Pätzold & Bird 1998), and without a full two-dimensional image of the structures being studied, it is difficult to draw inferences about geometry and structure.

We sought to address the issue of whether plumes actually extend to very high heliocentric altitudes by improving the signal-to-noise ratio in LASCO wide-field observations of the coronal hole and imaging the plumes in visible light as with previous, lower coronal observations.

Using a high-cadence observing sequence, we have generated LASCO C-3 images with effective exposure times of thousands of seconds and actual durations of less than 4 hr. These images, which are accumulated over a short enough time that polar plumes are not smeared by more than about one-fourth of their width, show that the brightest plumes extend to the outer edge of the LASCO C-3 field of view at 30 $R_{\odot}$ (in the image plane). We are able to estimate the excess electron density in the plumes and hence, using the global polar magnetic field, the β parameter within the plumes.[2]

2. OBSERVATION AND DATA REDUCTION

Because the LASCO C-3 field of view spans great variation in brightness, single images saturate the detector near the occulting disk after only 30 s of exposure, while there is still little or no signal from the outer portions of the coronal hole. Indeed, during the first few months of the *Solar and Heliospheric Observatory* (*SOHO*) mission, the LASCO synoptic images excluded the top and bottom parts of the image plane because individual images do not contain significant coronal signal. However, multiple exposures may be averaged together on the ground, where available dynamic range is virtually infinite, in order to increase the effective exposure time and bring extremely weak signals above the photon shot noise floor.

The practical limit to effective exposure time when viewing static structures is the longest acceptable time before solar rotation blurs the coronal image, reduced by the maximum duty cycle of the C-3 shutter. In 6 hr, the Sun rotates approximately 3°, which is sufficient to blur plumes tilted 45° out of the image plane by one-third of their apparent width; this may be regarded as a practical limit to acceptable exposure duration. The shutter duty cycle is determined by the ratio of the longest feasible exposure time to the fastest possible observing cadence. The cadence is limited by the telemetry resources available to LASCO. By reading out only half of the CCD and binning the C-3 images 2 × 2 to produce a 512 × 256 pixel image of the northern half of the corona, we were able to generate and downlink one 30 s losslessly compressed C-3 exposure approximately every 90–100 s, for a 30% duty cycle. Frame selection on the ground to avoid frames with missing data blocks and/or large cosmic ray hits further reduced the effective duty cycle to just over 20%. Lossy compression would have reduced the number of telemetered bits per frame, increasing the overall duty cycle of the exposure, but it would have discarded valuable information about the very structures we sought to identify.

On 1999 March 24, we ran a special observing sequence on LASCO for several hours using the program described above, yielding 3120 s of handpicked exposures during a single 4 hr period. The data were normalized for actual exposure time, despiked to remove stars as well as cosmic rays, and background subtracted with a smoothed monthly F-corona estimate generated from minimum image values in the surrounding 4 weeks, following the technique of Wu et al. (1997). For further enhancement, we transformed the data into the conformal azimuthal coordinates used by DeForest et al. (1997) and applied several spatial filters to the data to reduce the radial intensity gradient and enhance contrast for plumelike features.

The first filtering step on the transformed image was smoothing with a 4° (in azimuth) FWHM, circularly symmetric two-dimensional Gaussian kernel. This operation works well in the chosen conformal azimuthal coordinates because the scale factor between physical CCD pixels and transformed pixels changes with altitude, so that the outermost, faintest parts of the image are smoothed over more CCD pixels than are the innermost, brighter parts of the image. To maintain uniform feature contrast and eliminate the residual radial background gradient, we equalized the first and second moments of the brightness distribution across all horizontal rows in the transformed image. First we subtracted the average brightness value of each row from all the pixels in that row, then we divided the resulting brightness values by the standard deviation across the row. Finally, we subtracted out low spatial frequencies by one-dimensional unsharp masking: we subtracted a smoothed version of each row from the original data. The unsharp masking kernel was a one-dimensional Gaussian with an FWHM of 30° (in azimuth). The total effect of the processing was to limit resolved spatial structures to the 4°–30° range in azimuthal sizes and to over 10% in radius: only azimuthal structures that subtend more than 4° and less than 30° are seen, and radial resolution is limited to structures whose radial extent is more than 1/10 of the structure's distance from disk center.

Figure 1 shows the fully processed image in azimuthal space, complete with data from the LASCO C-2, High Altitude Observatory (HAO) Mk 3 K-Coronameter, and *SOHO* Extreme-Ultraviolet Imaging Telescope (EIT) instruments for context. The masked-out region near +30° azimuth is a foreground streamer that was removed from the final image. Several plumes are clearly visible, extending through the C-2 field of view and out to the edge of the C-3 field of view at 30 $R_{\odot}$ from disk center. Stars are not visible

[2] β, the dimensionless ratio of the gas dynamic pressure over the magnetic pressure, determines the degree of control that the magnetic field exerts over the plasma.

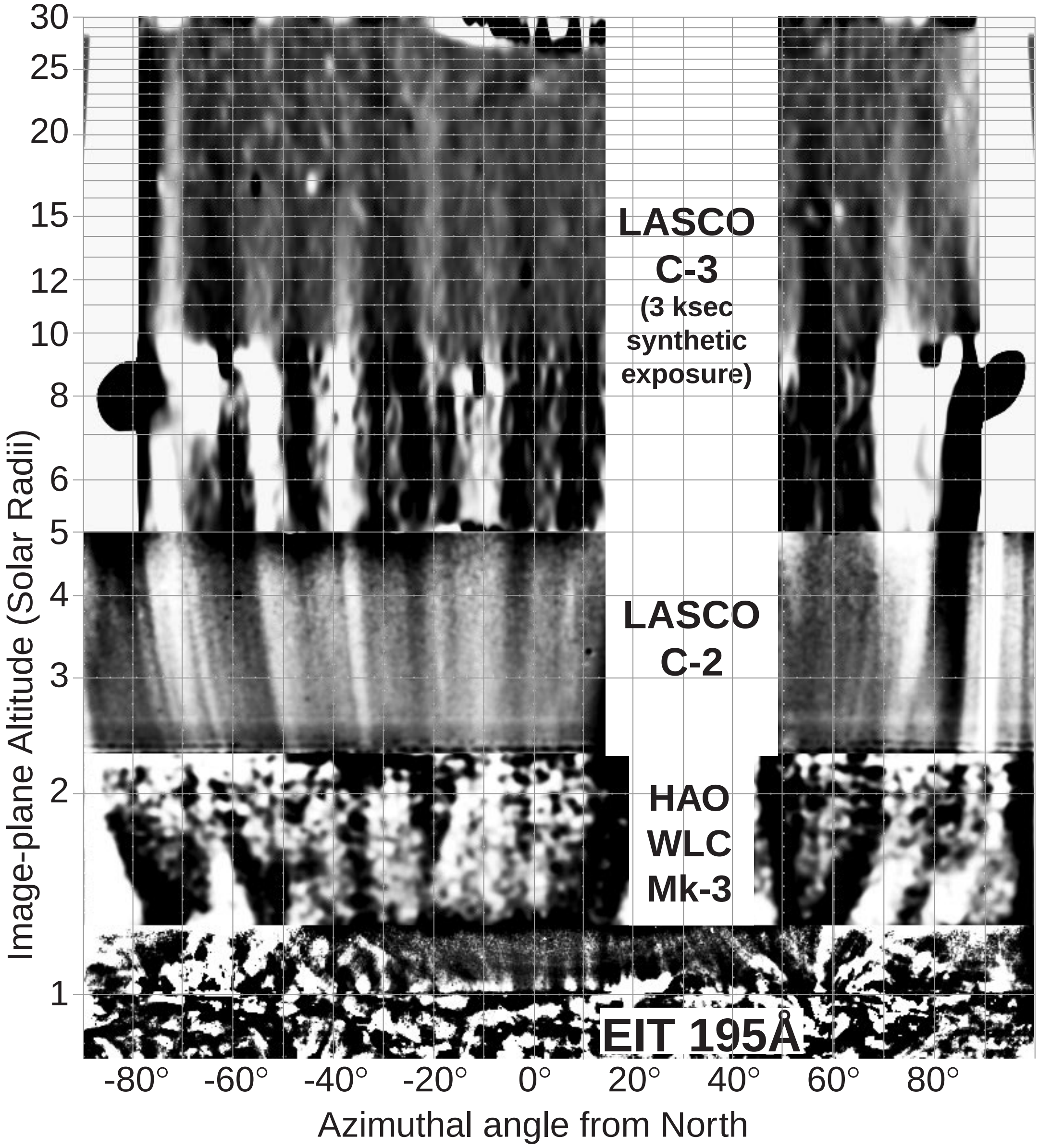

FIG. 1.—Polar plumes extending from the surface of the Sun out to 30 $R_{\odot}$ above the surface (in the image plane). Image is in conformal azimuthal coordinates. Vertical lines in image represent radial lines in normal space, and the radial direction is scaled logarithmically. Four instruments' data are presented. C-3, HAO K-Coronameter, and EIT images have been smoothed and detrended as described in text. C-2 image has been subjected only to radial filtering, to demonstrate by coalignment that the C-3 features are solar and not artificial.

in Figure 1, as they are in other published C-3 images, because they were filtered out in the despiking step. The HAO and EIT images are filtered by the same technique as the C-3 data (with a smaller smoothing kernel), but the C-2 data are only radial filtered and not unsharp masked. Figure 2 shows the C-3 data retransformed back to the original image plane, for context.

The use of unsharp masking, particularly in the presence of the foreground streamer, gave rise to the concern that the "plumes" in Figure 1 might in fact be artifacts of the filtering process. To address such concerns, we used smoothing and unsharp masking with Gaussian convolution kernels to prevent ringing of high spatial frequency components in the images, as can occur with boxcar or "top hat" kernels. As an additional check, the bases of the structures seen in the C-3 field correspond well with the bright structures at the top of the C-2 field of view, even though the C-3 images are unsharp masked and the C-2 images are not. This indicates that the C-3 structures are solar and not artificial in origin.

3. RESULTS

Figure 3 is a plot of the observed intensity in the plumes, in C-3 digitizer counts pixel^{-1} s^{-1}, versus azimuth for several altitudes in Figure 1. The plots show intensity that is zero-subtracted and unsharp masked but not radially filtered by standard deviation division as in Figures 1 and 2. The plumes visible in Figure 1 are also visible in the plot, with reduced contrast (as expected) at the higher altitudes. The lowest intensity plot, at 25 $R_{\odot}$ in the image plane, shows an intensity contrast of 0.2 counts pixel^{-1} s^{-1} peak-to-peak (under 0.1 counts pixel^{-1} s^{-1} rms). Because of the unsharp-masking and zero-subtraction steps that we used, no absolute contrast (plume brightness vs. background K-corona brightness) measurement is possible.

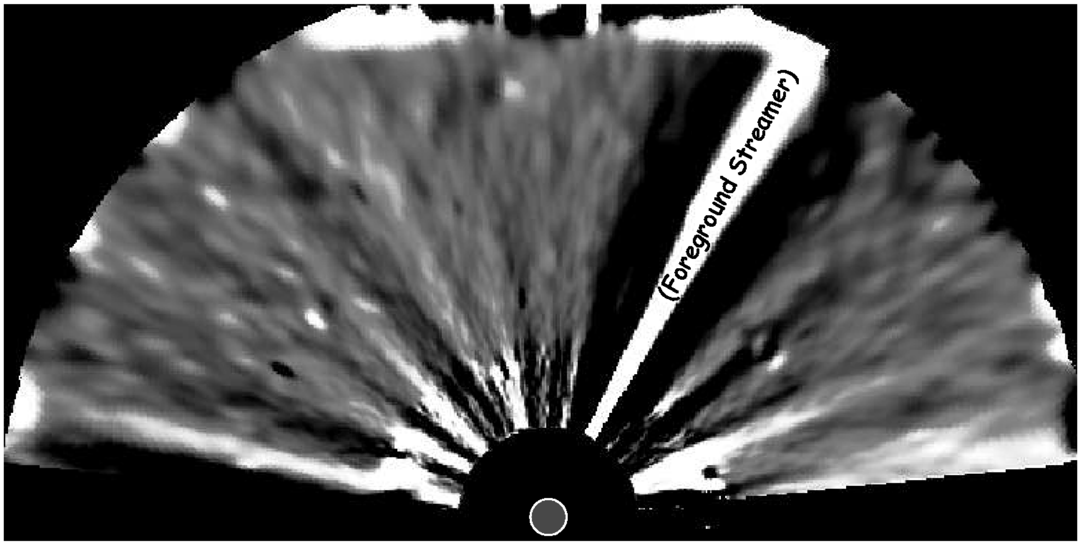

FIG. 2.—Outermost (C-3) portion of Fig. 1, transformed back into normal image coordinates. This is a processed, radially filtered image of the northern half of the C-3 field of view, showing actual appearance of the plumes as radial structures.

Figure 4*a* is a plot of measured brightness *along* each of three plumes (perpendicular to the plot in Figure 3), showing the excess brightness of these plumes compared to their adjacent interplume regions. Because mass is conserved in the solar wind, radial structures such as we observe at high altitude should fall off in density as R^{-2} if they support a constant-speed flow, or as $R^{-2}/V(R)$ if they support variable flow. Because LASCO C-3 sees primarily scattered light from the photosphere, with illumination decreasing as R^{-2} at high solar altitudes, the observed plume brightness falls more rapidly than the density falloff with altitude. Because the plasma is optically thin and the LASCO intensity signal is linear in the electron column density (modified by local illumination), the observed excess intensity of the scattered light in an imaged plume is proportional to the total excess column density in the plume. Neglecting brightness variations within the plume and using the radial geometry found in the outer corona (shown in Fig. 5),

$$I_{\text{plume}} = \frac{D}{\cos\phi} n'_e \sigma'_t B = \frac{R\alpha}{\cos\phi} \frac{v_0 n'_{e0} \pi}{v(R) R^2} \sigma'_t \frac{I_\odot}{R^2}, \quad (1)$$

where I_{plume} is the plume's excess brightness above background, D is the plume's diameter, ϕ is the plume's projection angle out of the plane of the sky, n'_e is the plume's

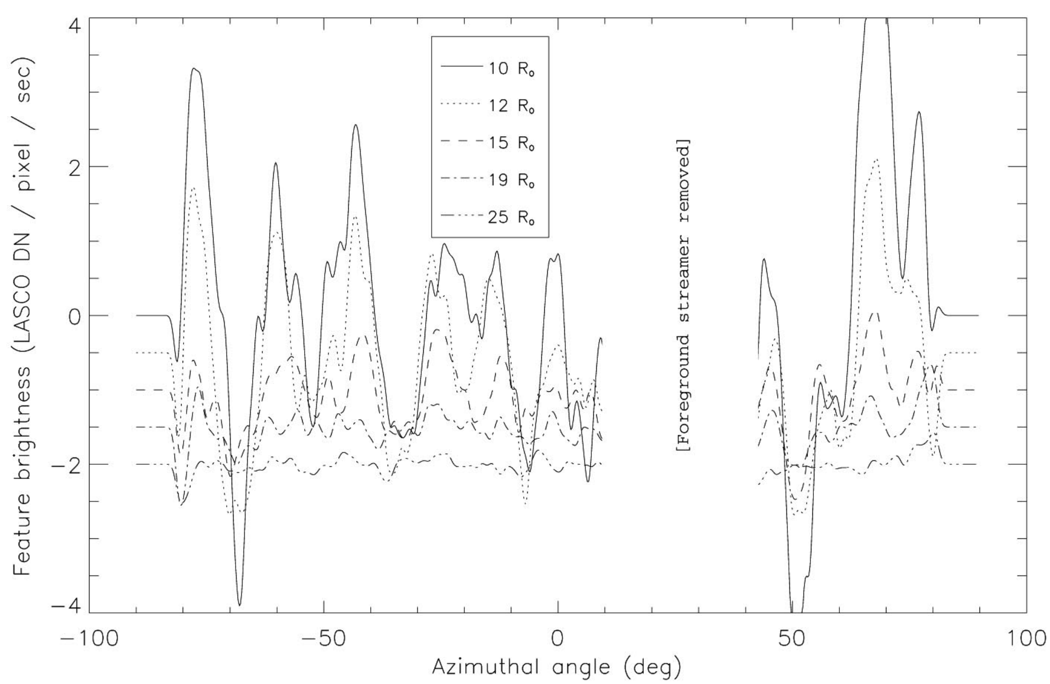

FIG. 3.—Plot of measured LASCO image intensity (in counts pixel^{-1} s^{-1}) vs. azimuth for several altitudes in Fig. 1. Plots are centered on zero because the data are unsharp masked, but have been offset for clarity. At the highest plotted image-plane altitude (25 ± 2 $R_\odot$), the plume-interplume contrast is approximately 0.2 counts pixel^{-1} s^{-1} peak-to-peak (0.07 counts pixel^{-1} s^{-1} rms).

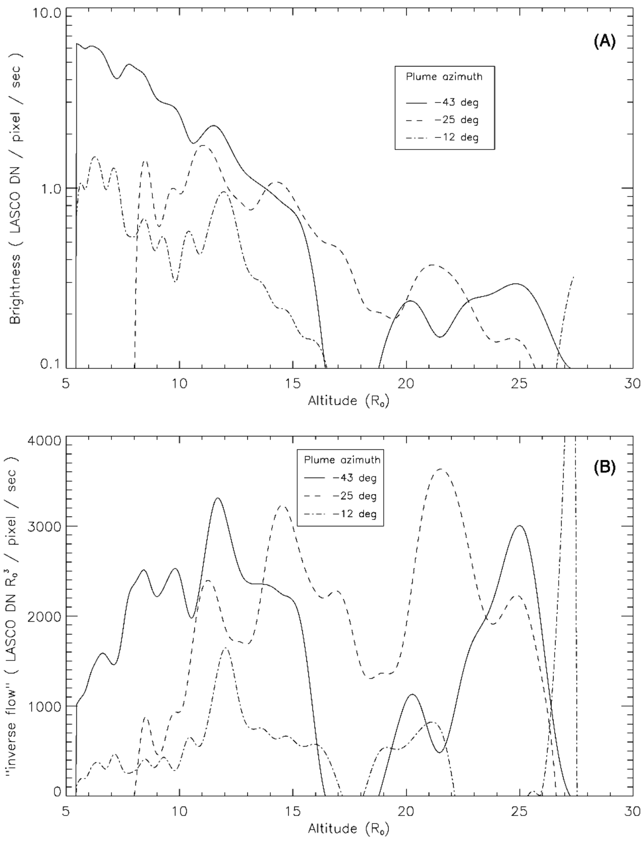

FIG. 4.—Plots of intensity (*a*) and flow-normalized intensity (*b*) measured at the LASCO focal plane vs. altitude in several of the plumes in Fig. 1. Flow-normalized intensity has been multiplied by b^3 to remove the effects of illumination and rarefaction in a constant-speed, radial-geometry wind (see text).

excess electron density over background, σ_t' is the differential Thomson scattering cross section [$\sigma_t' = \sigma_t(1 + \sin^2 \phi)(8\pi/3)$], B is the local illumination brightness, R is the actual radius along the plume from the Sun's center, α

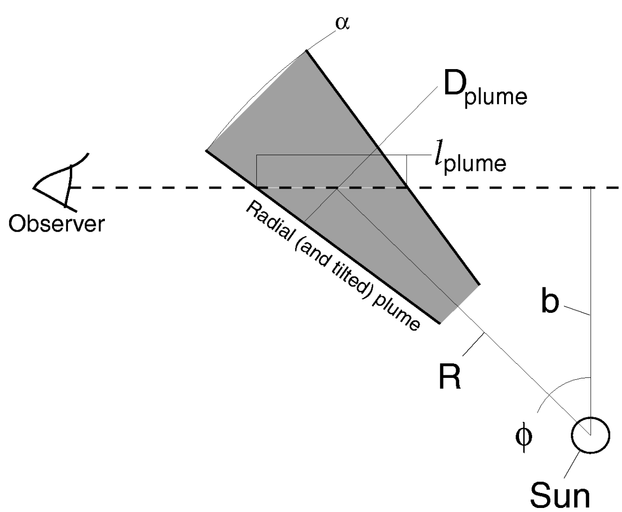

FIG. 5.—Idealized geometry of a radially expanding plume, used in the derivation of eqs. (1), (2), and (3) in the text. Plumes tilted out of the plane of the sky are seen at higher altitudes than is apparent on the image plane, an effect that is partially canceled out by the thicker cross section of the tilted plume along the line of sight and by the more favorable Thomson-scattering angle. Both effects increase the plume's visual contrast, while the higher three-dimensional altitude reduces it.

is the plume's subtended angle relative to the Sun's center, $v(R)$ is the outflow rate, n_{e0}' and v_0 are extrapolated values at 1 $R_\odot$, and $I_\odot$ is the Sun's surface brightness.

Collecting terms and converting to image-plane coordinates,

$$b^3 I_{\rm plume} = \left[\frac{\alpha \sigma_t' v_0 n_{e0}' I_\odot}{\cos^4 \phi}\right] \frac{1}{v(R)}, \tag{2}$$

where b is the impact parameter of the line of sight (in other words, radius from disk center in the image plane) and the quantity in square brackets is constant along each plume. The quantity $b^3 I_{\rm plume}$, plotted in Figure 4*b*, varies inversely as radial outflow speed. Figure 4*b* is consistent with either a rising or a decreasing trend with altitude, so this measurement does not indicate whether the wind in plumes is still undergoing acceleration at these altitudes.

Assuming that the plumes are visible only in Thomson-scattered photospheric light, and that they are circular in cross section (so that D, and hence α, may be measured by the apparent width of each plume), it is possible to invert equation (1) from the data and derive the excess density within the plumes using the LASCO photometric calibration. With a uniformly dense plume of thickness D and far enough from the Sun that $1/R \sim \sin(1/R)$, the plume's excess electron density at an observed point is

$$\begin{aligned} n_e' &= \frac{(I_{\rm plume}/I_\odot)(R^2/\pi)}{\sigma_t' s} \\ &= \frac{I_{\rm plume}}{I_\odot} \frac{16}{3\cos\phi(1+\sin^2\phi)} \frac{b^2}{\sigma_t D}, \end{aligned} \tag{3}$$

where s is the line-of-sight depth of the plume. With $D = 4$ $R_\odot$, $b = 30$ $R_\odot$, $I_{\rm plume} = 0.2$ counts pixel^{-1} s^{-1}, LASCO C-3 intensity calibration of 5×10^{-13} $I_\odot$ count^{-1} pixel^{-1} s^{-1}, and $\phi = 0$ (plume in the plane of the sky), we derive a "minimum" density excess of 2.6×10^3 cm^{-3} at 30 $R_\odot$. Using $\phi = 45°$, we derive a similar excess of 2.0×10^3 cm^{-3} at $R = 42$ $R_\odot$ or (assuming constant radial outflow) 3.9×10^3 cm^{-3} at $R = 30$ $R_\odot$. The a priori uncertainty in the typical density of our observed plumes is a factor of ~ 2 around these figures.

It is useful to normalize the observed densities relative to a constant-speed, radially expanding model wind. Conservation of mass requires that such wind decrease its density with altitude as R^{-2}; a factor of R^2 is multiplied back into the normalized "electron-flux density," yielding a figure that is comparable between measurements at different heliospheric distances (Feldman et al. 1996). Our estimated excess density values of $(2.6–4) \times 10^3$ cm^{-3} at $R = 30$ $R_\odot$ are equivalent to excess electron-flux densities of 51–77 cm^{-3} AU^2; this is 20–30 times more than the value of 2.5 cm^{-3} AU^2 measured by *Ulysses* for the total proton flux in the fast solar wind (Feldman et al. 1996) and a factor of 3–5 greater than the average total density of 800 cm^{-3} at 30 $R_\odot$ that was obtained by Bird et al. (1994) by radio sounding of the solar minimum coronal hole. The excess shows that plumes are significantly denser than the surrounding media at these altitudes. The plumes with the greatest observed azimuthal angle relative to the pole extend over 70° away from the pole in the plane of the sky (Fig. 1). If the plumes near the center of Figure 1 are inclined at that angle to the line of sight, then we are detecting them at actual altitudes as high as 80 $R_\odot$ in three-dimensional space.

We have calculated the plasma β parameter based on an assumed average value for the magnetic field in the coronal hole, an estimated temperature for the plumes, and the measured density. Neglecting differential-temperature effects between ions and electrons, the plasma β is

$$\beta = \frac{P_{\mathrm{gas}}}{P_{\mathrm{mag}}} \sim 2n_e k_{\mathrm{B}} T \frac{8\pi}{B^2}, \quad (4)$$

with k_{B} the Boltzmann constant, T the plasma temperature, and B the magnetic field strength. We approximate B by using the coronal hole average radial field of 10 G at the photosphere and applying superradial expansion and flux conservation. DeForest et al. (1997) observed plumes with a linear superradial expansion coefficient of 6 between the solar surface and 10 $R_{\odot}$, above which the plumes were approximately radial. Using this superradial expansion factor yields a total areal expansion of approximately 3×10^4 in the plumes' cross section between the surface and 30 $R_{\odot}$, for an estimated field strength of 3×10^{-4} G inside the plumes. Using $T = 10^6$K for the plume temperature yields a β of 200–300 at $R = 30\ R_{\odot}$. This should be regarded as an order-of-magnitude estimate, because of significant uncertainty in the magnetic field strength.

4. DISCUSSION

Our observation of plumes at three-dimensional altitudes of $\sim$30–45 $R_{\odot}$ supports the conclusion by Woo and Habbal (Woo 1996; Woo & Habbal 1997; Woo & Habbal 1998) that plume structures persist to at least 40 $R_{\odot}$, despite concerns (Pätzold & Bird 1998) about systematic errors in that radio sounding measurement. Our structures subtend approximately 10° relative to solar center, so they would take about 2.5 days to pass through the *Ulysses* beam at 4° day^{-1} (Pätzold & Bird 1998). This is somewhat longer than the 1 day period claimed by Woo & Habbal (1997), but the smoothing steps in our image preparation could prevent us from seeing a hypothetical signal at 4° azimuthal frequency, so our observation does not contradict the radio sounding results.

Because we are able to trace individual high-altitude plumes (even at azimuths, and hence colatitudes, as high as 70°) to root structures in the polar coronal holes within 20° of the pole, our data suggest that the "low-latitude plumes" detected by the Woo & Habbal (1997) measurement may in fact be polar plumes that expand superradially to low equivalent latitude at high altitudes. At altitudes above 5 $R_{\odot}$, plumes are approximately radial simply because they trace lines that are essentially straight and that have solar impact parameters of less than 1 $R_{\odot}$ (Fisher & Guhathakurta 1995): any linear feature is approximately radial at distances that are large compared to the feature's impact parameter with the origin.

Because of the faintness of the plume signal at high solar altitudes, we are able to detect only a few of the brightest plumes that were present on the day of our observation. The present result is that the very brightest plumes have overall azimuthal structure that extends to $\sim$45 $R_{\odot}$ in three dimensions, but we can draw no conclusion about what happens to the internal structure in the plumes. At 6 $R_{\odot}$ in the image plane (the top of the C-2 field of view), the brightest plumes have obvious internal structure, and fainter, smaller plumes are visible in the interstices between the brightest structures, but we have smoothed over such features in constructing the deep-field image with C-3. Hence, we cannot eliminate models that predict turbulent behavior or cross–field-line mixing of momentum or gas on spatial scales smaller than the width of a plume. Our observations eliminate only those that would cause the plumes themselves (on spatial scales of order 10° azimuth) to dissociate at altitudes below 30–45 $R_{\odot}$.

There are seven plumes visible at 20 $R_{\odot}$ in the image plane in the left half of Figure 2, each subtending approximately 5°–10° of azimuth. If the plumes are approximately circular in cross section (the assumption used for the density derivation above), then together they subtend $\sim$25 msr, or approximately 1% of the 3 sr subtended by the left half of the coronal hole. If their density is 10 times that of the surrounding medium and they are traveling at approximately the same speed as the overall wind, then these few brightest plumes alone account for about 10% of the mass flux in the fast solar wind emerging from their portion of the coronal hole, with more numerous but fainter plume structures presumably contributing 3–5 times more.

The existence of high-density streams 30–45 $R_{\odot}$ above the surface of the Sun does not negate instability models such as that of Parhi et al. (1999); rather, it both restricts the altitude range in which they can occur and lends strength to the argument that they do occur. Density fluctuations of an order of magnitude are not observed by *Ulysses* (Feldman et al. 1996), and fluid-dynamic instabilities remain the most credible model for explaining the disappearance of the observed density fluctuations between the top of the observable corona and the solar wind at 1 AU.

The lack of order-of-magnitude density fluctuations in the *Ulysses* measurements, coupled with the present observation, provides strong evidence for plume dissociation by mixing: if the plumes are not subject to mixing at high altitudes, then the disparity in density between plume and interplume regions must either be resolved by further superradial expansion of the plumes or be matched by an opposite disparity in outflow speed along the plumes to keep the outward mass flux constant across field lines. However, there is a known compositional mismatch between plumes, which have enhanced abundances of elements with low first-ionization potential, and the bulk of the high-speed solar wind, which does not (Feldman et al. 1998; Reisenfeld et al. 1999). Hence, the plumes cannot expand to form the bulk of the wind via very high altitude superradial expansion. Mixing or speed disparity must account for their disappearance.

In the absence of mixing across field lines, the plumes would have to move slowly at our observed altitudes and then be accelerated somewhere above 45 $R_{\odot}$ to match the outward flow of the interplume regions. If the interplume flow speed is 700 km s^{-1} and the interplume densities are to be consistent with *Ulysses*'s mass flux measurements, then in the absence of lateral mixing, the flow speed in the plumes would have to be only $\sim$40 km s^{-1} at 30–45 $R_{\odot}$ to match our observed excess densities. This speed is smaller than the observed wind speeds measured by direct tracers (Wood et al. 1999; Breen et al. 1999) and by Doppler dimming (Cranmer et al. 1999), implying that cross-field mixing, presumably due to turbulent instabilities in the plumes, is the most likely cause of the plumes' demise between 45 $R_{\odot}$ and 1 AU.

Our figure for the plasma β parameter within the plumes represents a lower bound estimate. We underestimated β by using only the *excess* density within the plumes, rather than the total density, to calculate the gas pressure. Due to the large amount of both spatial and temporal averaging that we have used to bring out the weak signal in the outer reaches of the C-3 field of view, the present measurement is not sensitive to such substructure at higher solar altitudes, but at the top of the LASCO C-2 field of view (6 $R_\odot$ in the image plane), the observed plumes have a considerable amount of substructure (Fig. 1). If the plumes are in fact as inhomogeneous at the top of the C-3 field of view as they are in the C-2 field, then D would be significantly reduced in equation (2), raising the peak density and β parameter estimates by another factor of perhaps 3–10 and reducing the filling factor estimates by a similar amount. Finally, pressure balance effects are likely to reduce the field strength in the plumes below the average for the coronal hole, increasing β further.

5. CONCLUSIONS AND SUMMARY

We have identified several bright polar plumes extending out to altitudes of 30 $R_\odot$ in the image plane, or $\sim 45\ R_\odot$ in three-dimensional space, well above the conventional top of the solar corona at 10 $R_\odot$ and into the constant-velocity wind regime as determined by interplanetary radio scintillation measurements (Breen et al. 1997; Breen et al. 1999). The plumes that we identify are imaged in white light, lending support to previous reports of high-altitude plume detection using radio sounding (Woo 1996). We are able to estimate the typical density enhancement in the plumes compared to the rest of the interplume corona and find values of a few 10^3 cm^{-3}, or R^2-normalized density excess of 50–80 cm^{-3} AU^2. Our values for plume density at these altitudes are significantly larger than the in situ R^2-normalized density for the solar wind as measured by *Ulysses* during its north polar pass. The discrepancy between the high observed plume densities at 30–45 $R_\odot$ and the uniformity of the interplanetary high-speed solar wind remains a puzzle. The present observation may be used to constrain the physics of the transition from inhomogeneous corona to homogeneous solar wind. We have demonstrated that high-altitude breakup of the plumes through hydrodynamic instabilities, such as are proposed by Parhi et al. (1999), is likely (in that $\beta \gg 1$) and that it is currently the most plausible explanation for the discrepancy between the coronal hole's inhomogeneity and the wind's uniformity.

We would like to thank the EIT Consortium for their willingness to interrupt the ongoing *SOHO*/EIT Synoptic Program to make this observation. We are also indebted to S. Suess of NASA/MSFC for helpful discussion of the results we present here. Comments from the referees and from A. Stern and W. Colwell at SWRI helped significantly to improve the write-up. C. E. D.'s work was supported through NASA grant NSG-5131. S. P. P. was supported through NASA contract S-8670-E. M. A. is supported through NASA grants and through the Naval Research Laboratory. *SOHO* is a mission of international collaboration between NASA and ESA.

REFERENCES

Ahmad, I. A., & Webb, D. F. 1978, Sol. Phys., 58, 323
Banerjee, D., Teriaca, L., Doyle, J. G., & Lemaire, P. 2000, Sol. Phys., 194, 43
Bird, M. K., et al. 1994, ApJ, 426, 373
Bohlin, J. D., Sheeley, N., & Tousey, R. 1975, in Space Research XV, ed. M. J. Rycroft (Berlin: Akademie), 651
Breen, A. G., et al. 1997, Adv. Space Res., 20, 27
———. 1999, J. Geophys. Res., 104, 9847
Brueckner, G. E., et al. 1995, Sol. Phys., 162, 357
Cranmer, S. R., et al. 1999, ApJ, 511, 481
DeForest, C. E. 1998, in Proc. Int. Meeting on Solar Jets and Coronal Plumes, ed. T. D. Guyenne (ESA SP-421; Noordwijk: ESA), 63
DeForest, C. E., et al. 1997, Sol. Phys., 175, 393
del Zanna, L., von Steiger, R., & Velli, M. 1998, Space Sci. Rev., 85, 349
Feldman, W. C., Barraclough, B. L., Phillips, J. L., & Wang, Y.-M. 1996, A&A, 316, 355
Feldman, U., Schüle, U., Widing, K., & Laming, J. M. 1998, ApJ, 505, 999
Fisher, R., & Guhathakurta, M. 1995, ApJ, 447, L139
Giordano, S., et al. 2000, ApJ, 531, L79
Habbal, S. R., Esser, R., Guhathakurta, M., & Fisher, R. 1995, Geophys. Res. Lett., 22, 1465
Kagashvili, E. K. H. 1999, ApJ, 512, 969
Kopp, R. A., & Holzer, T. E. 1976, Sol. Phys., 49, 43
Koutchmy, S. 1977, Sol. Phys., 51, 399
McComas, D. J., et al. 1995, in AIP Conf. Proc. 382, Solar Wind Eight, ed. D. Winterhalter (Woodbury: AIP), 44
Parhi, S., Suess, S. T., & Sulkanen, M. 1999, J. Geophys. Res., 104, 14781
Parker, E. N. 1958, ApJ, 128, 664
Pätzold, M., & Bird, M. K. 1998, Geophys. Res. Lett., 25, 1845
Poletto, G., et al. 1996, A&A, 316, 374
Reisenfeld, D. B., McComas, D. J., & Steinberg, J. T. 1999, Geophys. Res. Lett., 26, 1805
Saito, K. 1965, PASJ, 17, 421
Suess, S. T., Poletto, G., Wang, A.-H., Wu, S. T., & Cuseri, I. 1998, Sol. Phys., 180, 231
Walker, A. B. C., Jr., DeForest, C. E., Hoover, R. B., & Barbee, T. D. W., Jr. 1993, Sol. Phys., 148, 239
Walker, A. B. C., Jr., et al. 1988, Science, 241, 1781
Wang, Y.-M. 1994, ApJ, 435, L153
Woo, R. 1996, ApJ, 464, L95
Woo, R., & Habbal, S. R. 1997, Geophys. Res. Lett., 24, 1159
———. 1998, Geophys. Res. Lett., 25, 1849
Wood, B. E., et al. 1999, ApJ, 523, 444
Wu, S. T., et al. 1997, Sol. Phys., 175, 719